

Hafnium–Rhodium and Hafnium–Iridium Heterobimetallic Complexes Featuring the Bridging Germole Dianion Ligand $[\text{GeC}_4\text{Me}_4]^{2-}$

Jeffrey M. Dysard and T. Don Tilley*

Department of Chemistry, University of California at Berkeley,
Berkeley, California 94720-1460

Received March 10, 2000

The complex $[\text{Cp}^*(\eta^5\text{-C}_4\text{Me}_4\text{Ge})\text{HfMe}_2\text{Li}(\text{THF})]_2$ (**1**; $\text{Cp}^* = \text{C}_5\text{Me}_5$), prepared via treatment of $\text{Cp}^*\text{HfMe}_2\text{Cl}$ with 2 equiv of $\text{Li}[\text{C}_4\text{Me}_4\text{GeSiMe}_3]$, reacted rapidly with 2 equiv of $(\text{PMe}_3)_4\text{-RhOTf}$ ($\text{OTf} = \text{OSO}_2\text{CF}_3$) to give the novel Rh(III) zwitterionic complex *ansa*- $\{\eta^4\text{-C}_4\text{Me}_4\text{Ge}[\text{Rh}(\text{PMe}_3)_4\text{H}](\eta^5\text{-C}_5\text{Me}_4\text{CH}_2)\}\text{HfMe}_2$ (**2**), via loss of LiOTf . An intermediate in this reaction, presumed to be $\text{Cp}^*\{\eta^5\text{-C}_4\text{Me}_4\text{Ge}[\text{Rh}(\text{PMe}_3)_4]\}\text{HfMe}_2$ (**3**), was observed at low temperature by ^{31}P NMR spectroscopy. Reactions of **1** with $(\text{dmpe})_2\text{MOTf}$ ($\text{dmpe} = 1,2\text{-bis}(\text{dimethylphosphino})\text{ethane}$; $\text{M} = \text{Rh}, \text{Ir}$) produced the complexes $\text{Cp}^*\{\eta^5\text{-C}_4\text{Me}_4\text{Ge}[\text{Rh}(\text{dmpe})_2]\}\text{HfMe}_2$ (**5**) and $\text{Cp}^*\{\eta^5\text{-C}_4\text{Me}_4\text{Ge}[\text{Ir}(\text{dmpe})_2]\}\text{HfMe}_2$ (**6**), respectively. Complexes **5** and **6** possess the $[\text{GeC}_4\text{Me}_4]^{2-}$ ligand, which bridges the two metal atoms in a σ, π fashion.

Introduction

Recent interest in cyclic π -systems containing the heavier congeners of the group 14 elements¹ has motivated investigations of the chemistry of sila- and germacyclopentadienyl anions, and the corresponding silole and germole dianions.² These studies have included exploration of the transition-metal chemistry of these species, which has led to isolation of a η^5 -germoly complex of a transition metal, $[\text{Cp}^*\text{Ru}(\eta^5\text{-C}_4\text{Me}_4\text{GeSi}(\text{SiMe}_3)_3)]$,³ synthesis of the η^5 -silolyl complex $[\text{Cp}^*\text{Ru}(\eta^5\text{-C}_4\text{Me}_4\text{SiSi}(\text{SiMe}_3)_3)]$,⁴ and the isolation and structural characterization of η^5 -germoly and η^5 -silolyl d⁰ metal complexes.⁵ Recently we reported the synthesis and characterization of the aromatic germole dianion complex $[\text{Cp}^*(\eta^5\text{-C}_4\text{Me}_4\text{Ge})\text{HfMe}_2\text{Li}(\text{THF})]_2$ (**1**), which possesses a structure featuring Li ions coordinated in

both an η^1 and η^5 fashion by the germole dianion unit.⁶ The silylation of **1** produces the neutral germoly complex $[\text{Cp}^*(\eta^5\text{-C}_4\text{Me}_4\text{GeSiMe}_3)\text{HfMe}_2]$, which readily loses its $-\text{SiMe}_3$ group to regenerate the germole dianion complex.⁶ This reactivity, and the structure of the germole dianion complex, suggested that it might be possible to synthesize interesting heterobimetallic complexes⁷ in which the germole dianion $[\text{C}_4\text{Me}_4\text{Ge}]^{2-}$ serves as a bridging ligand. More specifically, we envisioned access to early–late bimetallic complexes via reaction of **1** with an electrophilic late-transition-metal fragment. Here we report the isolation of complexes containing a germole dianion bound to both early- and

(1) (a) Raabe, G.; Michl, J. *Chem. Rev.* **1985**, *85*, 419. (b) Raabe, G.; Michl, J. In *The Chemistry of Organic Silicon Compounds*; Patai, S., Rappoport, Z., Eds.; Wiley: New York, 1989; p 1102. (c) Apeloig, Y. In *The Chemistry of Organic Silicon Compounds*; Patai, S., Rappoport, Z., Eds.; Wiley: New York, 1989; p 151. (d) Brook, A. G.; Brook, M. A. *Adv. Organomet. Chem.* **1996**, *39*, 71. (e) Apeloig, Y.; Karni, M. In *The Chemistry of Organic Silicon Compounds*; Rappoport, Z., Apeloig, Y., Eds.; Wiley: New York, 1998; Vol. 2, Chapter 1. (f) Grützmacher, H. *Angew. Chem., Int. Ed. Engl.* **1995**, *34*, 295. (g) Denk, M.; Lennon, R.; Hayashi, R.; West, R.; Belyakov, A. V.; Verne, H. P.; Halland, A.; Bagner, M.; Metzler, N. *J. Am. Chem. Soc.* **1994**, *116*, 2691. (h) Heinemann, C.; Müller, T.; Apeloig, Y.; Schwarz, H. *J. Am. Chem. Soc.* **1996**, *118*, 2039. (i) Boehme, C.; Frenking, G. *J. Am. Chem. Soc.* **1996**, *118*, 2039. (j) Blakeman, P.; Gehrhuis, B.; Green, J. C.; Heinicke, J.; Lappert, M. F.; Kindermann, M.; Veszprémi, T. *J. Chem. Soc., Dalton Trans.* **1996**, 1275. (k) Heinemann, C.; Herrmann, W. A.; Thiel, W. *J. Organomet. Chem.* **1994**, *475*, 73. (l) Barton, T. J.; Banasiak, D. *J. Am. Chem. Soc.* **1977**, *99*, 5199. (m) Barton, T. J.; Burns, G. T. *J. Am. Chem. Soc.* **1978**, *100*, 5246. (n) Solouki, B.; Rosmus, P.; Bock, H.; Maier, G. *Angew. Chem., Int. Ed. Engl.* **1980**, *19*, 51. (o) Märkl, G.; Schlosser, W. *Angew. Chem., Int. Ed. Engl.* **1988**, *27*, 963. (p) Maier, G.; Mihm, G.; Reisenauer, H. P. *Angew. Chem., Int. Ed. Engl.* **1980**, *19*, 52. (q) Nakadaira, Y.; Sato, R.; Sakurai, H. *Organometallics* **1991**, *10*, 435. (r) Rich, J. D.; West, R. *J. Am. Chem. Soc.* **1982**, *104*, 6884. (s) Jutzi, P.; Meyer, M.; Dias, H. V. R.; Power, P. P. *J. Am. Chem. Soc.* **1990**, *112*, 4841. (t) Tokitoh, N.; Wakita, K.; Okazaki, R.; Nagase, S.; Schleyer, P. v. R.; Jiao, H. *J. Am. Chem. Soc.* **1997**, *119*, 6951. (u) Wakita, K.; Tokitoh, N.; Okazaki, R.; Nagase, S.; Schleyer, P. v. R.; Jiao, H. *J. Am. Chem. Soc.* **1999**, *121*, 11336.

(2) (a) Gordon, M. S.; Boudjouk, P.; Anwar, F. *J. Am. Chem. Soc.* **1983**, *105*, 4972. (b) Damewood, J. R. *J. Org. Chem.* **1986**, *51*, 5028. (c) Goldfuss, B.; Schleyer, P. v. R. *Organometallics* **1995**, *14*, 1553. (d) Hong, J.-J.; Boudjouk, P. *J. Am. Chem. Soc.* **1993**, *115*, 5883. (e) Curtis, M. D. *J. Am. Chem. Soc.* **1967**, *89*, 4241. (f) Curtis, M. K. *J. Am. Chem. Soc.* **1969**, *91*, 6011. (g) Jutzi, P.; Karl, A. *J. Organomet. Chem.* **1981**, *215*, 19. (h) Dufour, P.; Dubac, J.; Dartiguenave, M.; Dartiguenave, Y. *Organometallics* **1990**, *9*, 3001. (i) Freeman, W. P.; Tilley, T. D.; Arnold, F. P.; Rheingold, A. L.; Gantzel, P. K. *Angew. Chem., Int. Ed. Engl.* **1995**, *34*, 1887. (j) Freeman, W. P.; Tilley, T. D.; Liable-Sands, L. M.; Rheingold, A. L. *J. Am. Chem. Soc.* **1996**, *118*, 10457. (k) Joo, W.-C.; Hong, J.-H.; Choi, S.-B.; Kim, C. H. *J. Organomet. Chem.* **1990**, *391*, 27. (l) Boudjouk, P.; Castellino, S.; Hong, J.-H. *Organometallics* **1994**, *13*, 3387. (m) Hong, J.-H.; Boudjouk, P. *Bull. Soc. Chim. Fr.* **1995**, *132*, 495. (n) Sohn, H.; Bankwitz, U.; Powell, D. R.; West, R. *J. Organomet. Chem.* **1995**, *449*, C7. (o) Sohn, H.; Bankwitz, U.; Calabrese, J.; Apeloig, Y.; Müller, T.; West, R. *J. Am. Chem. Soc.* **1995**, *117*, 11608. (p) Freeman, W. P.; Tilley, T. D.; Yap, G. A. P.; Rheingold, A. L. *Angew. Chem., Int. Ed. Engl.* **1996**, *35*, 882. (q) West, R.; Sohn, H.; Powell, D. R.; Müller, T.; Apeloig, Y. *Angew. Chem., Int. Ed. Engl.* **1996**, *35*, 1002. (r) Goldfuss, B.; Schleyer, P. v. R.; Hampel, F. *Organometallics* **1996**, *15*, 1755. (3) Freeman, W. P.; Tilley, T. D.; Rheingold, A. L.; Ostrander, R. L. *Angew. Chem., Int. Ed. Engl.* **1993**, *32*, 1744. (4) Freeman, W. P.; Tilley, T. D.; Rheingold, A. L. *J. Am. Chem. Soc.* **1994**, *116*, 8428. (5) Dysard, J. M.; Tilley, T. D. *J. Am. Chem. Soc.* **1998**, *120*, 8245. (6) Dysard, J. M.; Tilley, T. D. *J. Am. Chem. Soc.* **2000**, *122*, 3097. (7) For recent reviews, see: (a) Abel, E. W.; Stone, F. G. A.; Wilkinson, G., Eds.; Pergamon: Oxford, U.K., 1995; Vol. 10. (b) Barlow, S.; O'Hare, D. *Chem. Rev.* **1997**, *97*, 647. (c) Hey-Hawkins, E. *Chem. Rev.* **1994**, *94*, 1661. (d) Stephan, D. W. *Coord. Chem. Rev.* **1989**, *95*, 41. (e) Bullock, R. M.; Casey, C. P. *Acc. Chem. Res.* **1987**, *20*, 167.

late-transition-metal centers and a rare example of structural characterization of a complex containing a Rh^I–Ge bond.⁸

Experimental Section

All manipulations were performed under an argon atmosphere using standard Schlenk techniques or a nitrogen-filled glovebox. Dry, oxygen-free solvents were employed throughout. Pentane, toluene, benzene, and diethyl ether were distilled from sodium/benzophenone, whereas benzene-*d*₆ and toluene-*d*₈ were distilled from Na/K alloy. The compounds [Cp*(η^5 -C₄Me₄Ge)HfMe₂Li(THF)]₂,⁶ (PMe₃)₄RhOTf,⁹ (dmpe)₂RhOTf,⁹ and (dmpe)₂IrOTf⁹ were prepared according to literature procedures. Me₃SiOTf was purchased from Aldrich Chemical Co. and distilled prior to use. NMR spectra were recorded at 300 or 500 MHz (¹H) with Bruker AMX-300 and DRX-500 spectrometers and at 125 MHz (¹³C{¹H}) or 202 MHz (³¹P{¹H}) with the DRX-500 spectrometer, at ambient temperature unless otherwise noted. Elemental analyses were performed by the microanalytical laboratory in the College of Chemistry at the University of California, Berkeley, CA. IR samples of solid materials were prepared as KBr pellets. All IR absorptions are reported in cm⁻¹ and were recorded with a Mattson Infinity 60 MI FTIR spectrometer.

ansa-{ η^4 -C₄Me₄Ge[Rh(PMe₃)₃H]}(η^5 -C₅Me₄CH₂)}HfMe₂ (2). A 100 mL Schlenk tube was charged with [Cp*(η^5 -C₄Me₄Ge)HfMe₂Li(THF)]₂ (0.257 g, 0.213 mmol) and 25 mL of benzene to generate a deep yellow solution. This solution was then added to a 100 mL round-bottom Schlenk flask containing (PMe₃)₄RhOTf (0.237 g, 0.426 mmol) in 50 mL of benzene to immediately produce a deep green solution. This reaction mixture was stirred for 30 min before the volatile materials were removed under dynamic vacuum. The remaining green residue was extracted with pentane (3 × 20 mL), and the combined pentane extracts were evaporated to give **2** as green crystals in 95% yield (0.359 g, 0.405 mmol). ¹H NMR (benzene-*d*₆, 500 MHz, 25 °C): δ 2.36 (s, 2 H, C₅Me₄CH₂), 2.28 (s, 6 H, C₄Me₄Ge), 2.18 (s, 6 H, C₄Me₄Ge), 1.96, 1.87 (s, 12 H, C₅Me₄CH₂), 1.23 (d, ²J_{HP} = 5 Hz, 18 H, PMe₃), 0.95 (d, ²J_{HP} = 5 Hz, 9 H, PMe₃), -0.48 (s, 6 H, HfMe₂), -9.70 (dm, J_{HRh} = 120 Hz, 1 H, RhH). ¹³C{¹H} NMR (500 MHz, benzene-*d*₆, 25 °C): δ 140, 110 (s, C₄Me₄Ge) 131, 119, 113 (s, C₅Me₄CH₂), 41.1 (s, HfMe₂), 26.4 (s, CH₂), 22.5 (bm, 3 PMe₃), 22.5, 16.8, 13.0, 12.0 (s, C₄Me₄Ge and C₅Me₅). ³¹P{¹H} NMR (202 MHz, benzene-*d*₆, 25 °C): δ -11.6 (dd, J_{PRh} = 152 Hz, ²J_{PP} = 32 Hz, 2 P, Rh(PMe₃)₂), -15.3 (dt, J_{PRh} = 119 Hz, ²J_{PP} = 32 Hz, 1 P, Rh(PMe₃)). Anal. Calcd for C₂₉H₆₀GeHfP₃Rh: C, 40.70, H, 7.01. Found: C, 40.35, H, 7.09. IR (cm⁻¹): 2974 s, 2904 s, 2868 s, 1858 m (Rh–H), 1420 m, 1294 m, 1621 w, 1140 w, 1094 w, 945 s, 850 w, 747 w, 668 w. Mp: 95 °C dec.

Cp*{ η^5 -C₄Me₄Ge[Rh(dmpe)₂]}HfMe₂ (5). A 100 mL Schlenk tube was charged with [Cp*(η^5 -C₄Me₄Ge)HfMe₂Li(THF)]₂ (0.099 g, 0.082 mmol) and 25 mL of benzene to give a deep yellow solution. This solution was then added to a 100 mL round-bottom Schlenk flask containing (dmpe)₂RhOTf (0.091 g, 0.164 mmol) in 50 mL of benzene, resulting in a deep red solution. This reaction mixture was stirred for 30 min before the volatile materials were removed under dynamic vacuum. The remaining red-orange residue was extracted with toluene (3 × 20 mL). The combined extracts were

concentrated to 10 mL and cooled to -35 °C to give **5** as red-orange needles in 83% yield (0.126 g, 0.136 mmol). ¹H NMR (benzene-*d*₆, 500 MHz, 25 °C): δ 2.43 (s, 6 H, C₄Me₄Ge), 2.39 (s, 6 H, C₄Me₄Ge), 2.19 (s, 15 H, C₅Me₅), 1.37 (bs, 8 H, Me₂-PCH₂CH₂PMe₂), 1.14 (bs, 24 H, Me₂PCH₂CH₂PMe₂), -0.470 (s, 6 H, HfMe₂). ¹³C{¹H} NMR (500 MHz, benzene-*d*₆, 25 °C): δ 151, 127 (s, C₄Me₄Ge), 116 (s, C₅Me₅), 40.8 (s, HfMe₂), 33.4 (m, Me₂PCH₂CH₂PMe₂), 24.1 (m, Me₂PCH₂CH₂PMe₂), 21.6, 17.3 (s, C₄Me₄Ge), 13.3 (s, C₅Me₅). ³¹P{¹H} NMR (202 MHz, benzene-*d*₆, 25 °C): δ -33.4 (d, J_{PRh} = 123 Hz, Me₂PCH₂-CH₂PMe₂). Anal. Calcd for C₃₂H₆₅GeHfP₄Rh: C, 41.43, H, 7.06. Found: C, 41.04, H, 7.41. IR (cm⁻¹): 2950 s, 2898 s, 1419 m, 1293 m, 1274 m, 1261 m, 1177 w, 1100 w, 1021 w, 933 m, 841 w, 807 w. Mp: 155–159 °C.

Cp*{ η^5 -C₄Me₄Ge[Ir(dmpe)₂]}HfMe₂ (6). A 100 mL Schlenk tube was charged with [Cp*(η^5 -C₄Me₄Ge)HfMe₂Li(THF)]₂ (0.236 g, 0.196 mmol) and 25 mL of benzene to give a deep yellow solution. This solution was then added to a 100 mL round-bottom Schlenk flask containing (dmpe)₂IrOTf (0.251 g, 0.392 mmol) in 50 mL of benzene. The resulting light red solution was stirred for 30 min before the volatile materials were removed under dynamic vacuum. The remaining red residue was extracted with toluene (3 × 20 mL). The combined extracts were concentrated to 10 mL and cooled to -35 °C to give **6** as an orange powder in 87% yield (0.346 g, 0.340 mmol). ¹H NMR (benzene-*d*₆, 500 MHz, 25 °C): δ 2.40 (s, 6 H, C₄Me₄Ge), 2.35 (s, 6 H, C₄Me₄Ge), 2.15 (s, 15 H, C₅Me₅), 1.56 (bs, 8 H, Me₂-PCH₂CH₂PMe₂), 1.15 (bs, 24 H, Me₂PCH₂CH₂PMe₂), -0.440 (s, 6 H, HfMe₂). ¹³C{¹H} NMR (500 MHz, benzene-*d*₆, 25 °C): δ 143, 124 (s, C₄Me₄Ge), 116 (s, C₅Me₅), 40.2 (s, HfMe₂), 34.8 (m, Me₂PCH₂CH₂PMe₂), 26.1 (m, Me₂PCH₂CH₂PMe₂), 20.7, 17.0 (s, C₄Me₄Ge), 13.0 (s, C₅Me₅). ³¹P{¹H} NMR (202 MHz, benzene-*d*₆, 25 °C): δ 0.315 (s, Me₂PCH₂CH₂PMe₂). Anal. Calcd for C₃₂H₆₅GeHfP₄Ir: C, 37.79, H, 6.44. Found: C, 38.10, H, 6.26. IR (cm⁻¹): 2968 s, 2909 s, 1998 w, 1420 m, 1375 w, 1293 w, 1122 w, 1078 w, 933 m, 845 w, 723 w, 651 w. Mp: 180 °C dec.

X-ray Crystallography. Red-orange, platelike crystals were obtained from a concentrated toluene solution at -35 °C. A crystal of dimensions 0.62 × 0.19 × 0.04 mm was mounted on a glass fiber using Paratone-N hydrocarbon oil. Data were collected using a Siemens SMART diffractometer with a CCD area detector. A preliminary orientation matrix and unit cell parameters were determined by collecting 60 10 s frames, followed by spot integration and least-squares refinement. A hemisphere of data was collected using ω scans of 0.3°. Frame data were integrated (*xy* spot spread 1.60°; *z* spot spread 0.60°) using the program SAINT (SAX area detector integration program, version 4.024; Siemens Industrial Automation, Inc., Madison, WI, 1995). The data were corrected for Lorentz and polarization effects. An absorption correction was performed using SADABS (*T*_{max} = 0.9765, *T*_{min} = 0.3466). The 37 143 integrated reflections were averaged in point group 2/*m* to give 15 003 unique reflections (*R*_{int} = 0.076), but only 7136 reflections were considered observed (*I* > 3.00σ(*I*)). No decay correction was necessary. Inspection of the systematic absences uniquely defined the space group as *P*2₁/*n*. The structure was solved using direct methods (SIR92) and refined by full-matrix least-squares methods using *teXsan* software. Only one of the two independent molecules in the unit cell is displayed in Figure 1. The non-hydrogen atoms were refined anisotropically in both molecules. The number of variable parameters was 703, giving a data/parameter ratio of 10.15. The maximum and minimum peaks on the final difference Fourier map corresponded to 2.34 and -7.33 e/Å³. *R* = 0.052, *R*_w = 0.056, GOF = 1.38. The crystallographic data are summarized in Table 1.

Results and Discussion

Initial reactivity studies focused on attempts to coordinate a transition-metal fragment to the germole

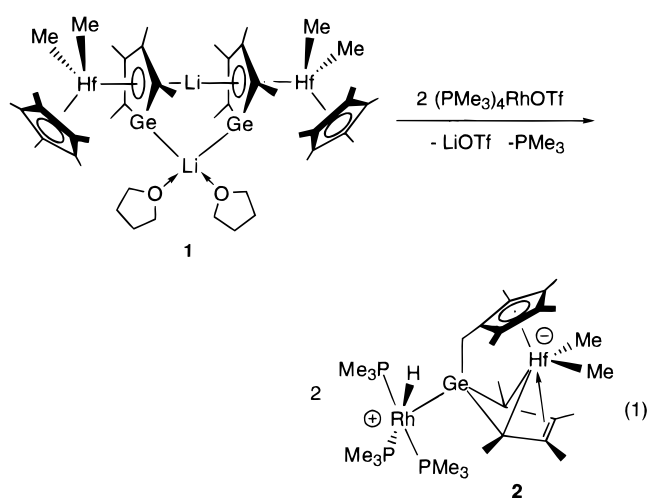
(8) A keyword search for complexes containing Rh and Ge in the Cambridge Structural Database as well as the Web of Science returned no examples of structurally characterized compounds with a Rh^I–Ge bond. However, the related germylene complex *cis*-[RhCl{Ge(N(SiMe₃)₂)}₂](PPh₃)₂, mentioned only in review, was structurally characterized as possessing a Ge...Cl interaction (Lappert, M. F.; Rowe, R. S. *Coord. Chem. Rev.* **1990**, *100*, 267).

(9) (a) Thorn, D. L. *Organometallics* **1982**, *1*, 197. (b) Thorn, D. L. *Organometallics* **1985**, *4*, 192. (c) Aizenberg, M.; Milstein, D. *J. Chem. Soc., Chem. Commun.* **1994**, 411.

Table 1. Summary of Crystallographic Data

empirical formula	RhHfP ₄ GeC ₃₂ H ₆₅
fw	927.75
cryst color, habit	red-orange, platelike
cryst dimens	0.62 × 0.19 × 0.04 mm
cryst syst	monoclinic
cell determ (2θ range)	8192 (4.0–45.0°)
lattice params	
<i>a</i>	23.7258(2) Å
<i>b</i>	15.0198(2) Å
<i>c</i>	24.2155(2) Å
β	117.0811°
<i>V</i>	7683.3(1) Å ³
space group	<i>P</i> 2 ₁ / <i>n</i> (No. 14)
<i>Z</i>	8
<i>D</i> _{calc}	1.604 g/cm ³
μ(Mo Kα)	40.77 cm ^{−1}
diffractometer	Siemens SMART
radiation	MoKα (λ = 0.710 69 Å), graphite monochromated
temp	−105 °C
scan type	ω (0.3° per frame)
no. of rflns measd	total, 37 143; unique, 15 003 (<i>R</i> _{int} = 0.076)
no. of observns (<i>I</i> > 3.00σ(<i>I</i>))	7136
structure soln	direct methods (SIR92)
refinement	full-matrix least squares
residuals: <i>R</i> ; <i>R</i> _w	0.052; 0.056
max peak in final diff map	2.34 e/Å ³
min peak in final diff map	−7.33 e/Å ³

ring of [Cp*(η^5 -C₄Me₄Ge)HfMe₂Li(THF)]₂ (**1**)⁶ with formation of a “sandwich” structure. This possibility is suggested by the structure of **1**, which features a lithium atom coordinated in an η^5 fashion by the germole rings of two [Cp*(η^5 -C₄Me₄Ge)HfMe₂][−] anions. However, reaction of **1** with FeCl₂, FeCl₂(THT) (THT = tetrahydrothiophene) (in benzene, toluene, or THF), or ¹/₄ [Cp*RuCl]₄¹⁰ (in THF or toluene) resulted only in complex mixtures of products. In contrast, the reaction of **1** with 2 equiv of (PMe₃)₄RhOTf⁹ at room temperature in benzene resulted in loss of LiOTf with formation of an intensely colored green solution. The soluble product from this reaction, isolated as green crystals from pentane in 95% yield, is the unusual zwitterionic *ansa*-{ η^4 -C₄Me₄Ge[Rh(PMe₃)₃H](η^5 -C₅Me₄CH₂)}HfMe₂ (**2**; eq 1).



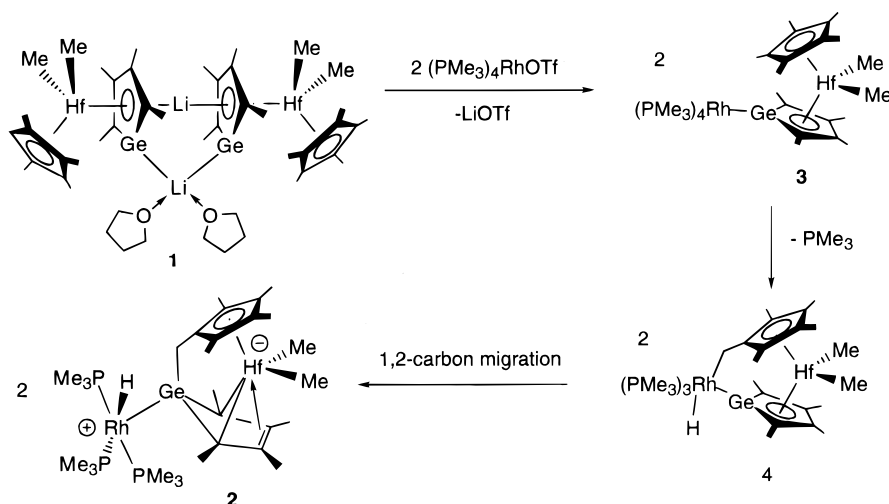
The ¹H NMR spectrum of **2** exhibits a characteristic shift for the Hf–Me protons at δ −0.48, along with

resonances at δ 0.95 and 1.23 for two different types of PMe₃ ligands. The activated Cp* group gives rise to three singlets in a 6:6:2 ratio at δ 1.87, 1.96, and 2.36, respectively, while the η^4 -germole group is associated with two methyl peaks at δ 2.28 and 2.36. Notably, the absence of coupling between Rh and the methylene hydrogens bound to Ge indicates that rhodium is not bonded to the CH₂C₅Me₄ fragment. There is a Rh–H resonance at δ −9.70 which appears as a doublet of multiplets coupled to both Rh (*J*_{RhH} = 120 Hz) and inequivalent phosphorus atoms (*J*_{HP} = 15 Hz, *J*_{H–2P} = 25 Hz). The ³¹P NMR spectrum of **2** displays two separate resonances for the different kinds of phosphine ligands at δ −11.6 (dd, *J*_{PRh} = 152 Hz, ²*J*_{PP} = 32 Hz, 2 P, Rh(PMe₃)₂) and −15.3 (dt, *J*_{PRh} = 119 Hz, ²*J*_{PP} = 32 Hz, 1 P, Rh(PMe₃)). The spectroscopic data for **2** are consistent with a square-pyramidal coordination geometry for Rh, with apical coordination of the germanium atom, and this structure was confirmed by X-ray crystallography (vide infra). Also, the ¹³C NMR spectrum of **2** exhibits two distinct shifts for the ring carbons of the germole ring at 110 and 140 ppm. X-ray-quality crystals of **2** were obtained by cooling a concentrated pentane solution to −30 °C. Although X-ray crystallography confirmed the connectivity and main structural features for **2**, including the η^4 -coordination of the germole unit, the refinement of accurate metric parameters was not possible, due to a poor data set.

A possible mechanism for the formation of **2** is given in Scheme 1. Presumably, the initial step in this reaction is nucleophilic attack on the Rh center by the germole anion complex to give a new Rh–Ge-bonded species (**3**). The formation of **3** is supported by low-temperature NMR spectra of the reaction mixture. Treatment of **1** with 2 equiv of (PMe₃)₄RhOTf at −78 °C in toluene-*d*₈ resulted in formation of a red solution (rather than a green solution as observed at room temperature). Although attempts to isolate a product from such solutions failed, the ³¹P NMR spectrum at −70 °C revealed clean formation of an intermediate, giving rise to two complex multiplets at δ −5.2 and −32. As the solution is warmed, these two multiplets broaden and eventually coalesce at −20 °C into a doublet (δ −20, *J*_{PRh} = 146 Hz), which would be expected for **3** if all of the PMe₃ ligands were rendered equivalent on the NMR time scale. The ¹H NMR spectrum of **3** at −70 °C revealed the presence of equivalent Hf–Me groups, which resonate at δ −0.40, and additional resonances at δ 2.2 for the Cp* ligand and at δ 2.4 and 2.6 for the Me groups of the germole ring. As the solution was warmed from −70 to −20 °C, the ¹H NMR spectrum remained virtually unchanged, except that the PMe₃ resonances broadened and coalesced into one broad peak at ca. δ 1.3. The coalescence observed in the variable-temperature NMR spectra for compound **3** may be attributed to dynamic behavior involving rotation of a trigonal bipyramidal P₄Rh group about the Rh–Ge bond or Berry pseudorotation at the Rh center. Both of these processes would preserve the mirror plane symmetry (equivalent HfMe groups) observed in the ¹H NMR spectra. At 0 °C the doublet attributed to **2** and free PMe₃ grew in with no evidence for intermediate **4**. Presumably, **3** loses a PMe₃ ligand from the Rh(I) center to form

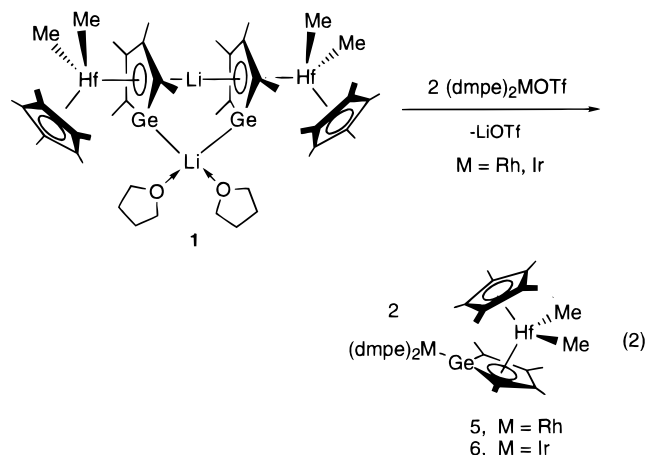
(10) Fagan, P. J.; Ward, M. D.; Caspar, J. V.; Calabrese, J. C.; Krusic, P. J. *J. Am. Chem. Soc.* **1988**, *110*, 2981.

Scheme 1



a coordinately unsaturated, 16-electron complex which oxidatively adds a C–H bond of the Cp* ligand to generate a new 18-electron, pseudo-octahedral Rh(III) center (**4**). A 1,2-carbon migration of the metalated CH₂ group from Rh to germanium would result in the formation of **2**, containing square-pyramidal Rh(III) and d⁰ hafnium centers. This last step, the generation of a diene complex of the germole unit, has previously been observed in different reactions of **1**.⁶

To isolate a complex analogous to the proposed intermediate **3**, we employed the rhodium triflate (dmpe)₂RhOTf⁹ possessing relatively nonlabile phosphine ligands. In fact, reaction of **1** with 2 equiv of (dmpe)₂RhOTf at room temperature in benzene resulted in formation of the new (η⁵-germole)hafnium complex Cp*{η⁵-C₄Me₄Ge[Rh(dmpe)₂]}HfMe₂ (**5**) in 83% yield after crystallization from toluene at –35 °C (eq 2).



Compound **5** is quite thermally stable, as heating a toluene solution to 140 °C for 24 h resulted in no detectable decomposition.

The ¹H NMR spectrum of **5** exhibits a characteristic Hf–Me peak at δ –0.47, a Cp* resonance at δ 2.20, and two peaks for the germole ring methyl protons at δ 2.39 and 2.43. In addition, there are two very broad resonances at δ 1.15 and 1.37 for the dmpe ligands, which resonate as a sharp doublet (*J*_{P–Rh} = 123 Hz) in the ³¹P NMR spectrum. Finally, the ¹³C NMR shifts for the ring

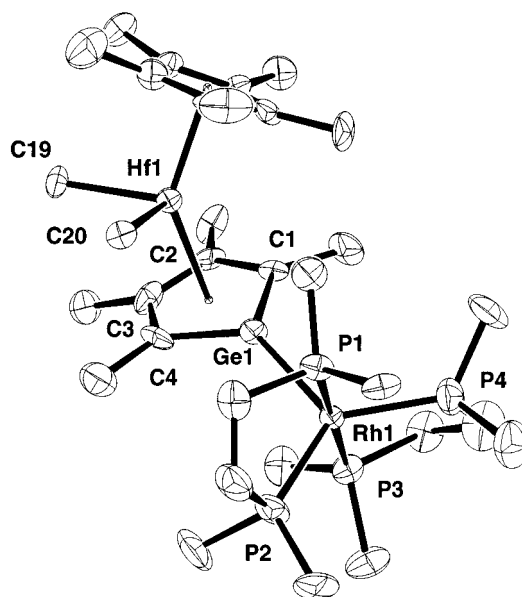


Figure 1. ORTEP diagram of Cp*{η⁵-C₄Me₄Ge[Rh(dmpe)₂]}HfMe₂ (**5**).

carbons of the germole ring (δ 127 and 151) lie in a region consistent with η⁵ coordination of the germole unit.⁶

X-ray-quality crystals of **5** were grown by slow cooling of a concentrated toluene solution to –35 °C, and the molecular structure of one of the two independent molecules in the unit cell is shown in Figure 1. The molecular structure of **5** is typical of bent metallocene derivatives of hafnium and is analogous to the previously reported structure for Cp*{η⁵-C₄Me₄GeSiMe₃}-HfCl₂.⁵ The Rh-containing portion of **5** adopts a trigonal-bipyramidal geometry with the Ge atom of the germole ring, P2, and P4 occupying the equatorial positions. The Ge–C bond lengths (1.92(1) and 1.95(2) Å; Table 2) are short relative to the analogous germanium–carbon bonds in localized germole anions (1.957(7)–2.007(9) Å).^{2j} The C–C bonds in the germole ring are roughly equivalent (1.48(2), 1.43(2), and 1.43(2) Å) and are comparable to those found in **1** (1.42(2), 1.40(2), and 1.43(2) Å), suggesting an aromatic η⁵-germole ligand. Compound **5**, which represents the first structurally characterized complex possessing an unambiguous Rh^I–

Table 2. Selected Interatomic Distances (Å) and Angles (deg) for **5**

(a) Bond Distances			
Hf(1)–Ge(1)	2.963(2)	Ge(1)–C(1)	1.92(1)
Hf(1)–Ge ^{*a}	2.3000(6)	Ge(1)–C(4)	1.95(2)
Hf(1)–Cp ^{*a}	2.2702(6)	C(1)–C(2)	1.48(2)
Hf(1)–C(19)	2.29(1)	C(2)–C(3)	1.43(2)
Hf(1)–C(20)	2.30(1)	C(3)–C(4)	1.43(2)
Rh(1)–Ge(1)	2.488(2)	Rh(1)–P(1)	2.273(4)
Rh(1)–P(2)	2.273(4)		
(b) Bond Angles			
Ge [*] –Hf(1)–Cp [*]	137.80(3)	C(19)–Hf(1)–C(20)	89.2(5)
P(1)–Rh(1)–Ge(1)	94.1(1)	P(2)–Rh(1)–Ge(1)	113.1(1)
Ge [*] –Ge(1)–Rh(1)	155.24	C(1)–Ge(1)–C(4)	86.9(6)

^a Ge^{*} and Cp^{*} denote the centroids of the germolyl and Cp^{*} rings, respectively.

Ge single bond, exhibits a Rh–Ge bond length of 2.488-(2) Å. Finally, the Cp^{*}(centroid)–Hf distance (2.27 Å), the germole(centroid)–Hf distance (2.30 Å), and the germole–Hf–Cp^{*} angle (137.8°) are comparable to those found in Cp^{*}[η^5 -C₄Me₄GeSiMe₃]HfCl₂ (2.22 Å, 2.33 Å, and 136.1°, respectively).⁵

Surprisingly, the analogous reaction of **1** with 2 equiv of (PMe₃)₄IrOTf⁹ (in benzene, toluene, or THF) was not clean, and in each case a mixture of products was observed, none of which possessed an Ir–H bond (by ¹H NMR spectroscopy). However, reaction of **1** with 2 equiv of (dmpe)₂IrOTf⁹ at room temperature in benzene resulted in clean formation of Cp^{*}{ η^5 -C₄Me₄Ge[Ir-(dmpe)₂]}HfMe₂ (**6**) in 87% yield after crystallization from toluene. The characterization of **6** is based largely

on comparisons of spectroscopic data with those for **5**. The ³¹P NMR spectrum of **6** exhibits one sharp singlet for all four dmpe phosphorus atoms at δ 0.32. In addition, as for **5**, the ¹³C NMR spectrum of **6** exhibits peaks for the germolyl ring carbons (δ 143 and 124) in a region consistent with η^5 coordination.

In summary, we have observed heterobimetallic complexes containing an η^5 -germole dianion as a bridging ligand. In one of these systems, C–H activation and 1,2-migration generate an unusual zwitterion containing cationic Rh(III) and anionic Hf(IV) centers. In addition, early–late-transition-metal complexes containing a germole dianion bound both in an η^5 fashion to d⁰ hafnium and in an η^1 fashion to either Rh(I) or Ir(I) were synthesized. Future investigations will focus on both the reaction chemistry of these complexes and the synthesis of new compounds in which the germole dianion is “sandwiched” in an η^5 manner between two transition metals.

Acknowledgment is made to the National Science Foundation of their generous support of this work. We thank Dr. Fred Hollander for assistance with the X-ray structure determinations.

Supporting Information Available: Tables of crystal, data collection, and refinement parameters, bond distances and angles, and anisotropic displacement parameters for **5**. This material is available free of charge via the Internet at <http://pubs.acs.org>.

OM000220L